Consequences of Modulated Precompression along Reaction Coordinates. Synthesis, Crystallographic Structural Studies, and Rate of Intramolecular Dyotropy in an Extended Series of *syn*-Sesquinorbornene Disulfones

George A. O'Doherty,[1] Robin D. Rogers,[2] and Leo A. Paquette*

Contribution from the Evans Chemical Laboratories, The Ohio State University, Columbus, Ohio 43210, and the Department of Chemistry, Northern Illinois University, DeKalb, Illinois 60115

Received July 26, 1993[⊗]

Abstract: In order to produce a broad range of *syn*-sesquinorbornene disulfones, (Z)-1,2-bis(phenylsulfonyl)ethylene was added in Diels–Alder fashion (high-pressure conditions) to tricyclo[5.2.1.$0^{2,6}$]deca-2,5,8-trienes carrying isopropylidene or spirocyclopropane subunits at one or two sites. The central double bond in these adducts was then regiospecifically reduced with diimide, epoxidized with MCPBA, or cyclopropanated by [3 + 2] cycloaddition with diazomethane and subsequent photoinduced nitrogen extrusion. Each product in all three series was subjected to X-ray crystallographic analysis in order to quantify in the solid state the distance which each endo α-sulfonyl proton is required to traverse during dyotropic migration to the proximal norbornene double bond. The kinetics of these isomerizations were also determined, a relative reactivity scale was realized, and the values of k_{rel} at 160 °C were found not to correlate well with the average distance across the intracavity gap. Although proximity of the reaction centers is clearly a prerequisite for smooth operation of the dyotropic shifts, modulation of this distance is not the sole contributor to reaction rate. Rather, the data are in agreement with the working hypothesis that various levels of steric compression within these disulfones facilitate passage over the relevant transition state to a greater or lesser degree depending on the magnitude of these nonbonded interactions.

The ability of enzymes to catalyze reactions rests on their heightened capacity for effecting key differences in the levels of interaction with the initial state of the reactant and those specifically available to the transition state.[3] The resultant changes in enthalpy and entropy are most often implemented through hydrogen-bonding schemes that have the consequence of providing highly advantageous spatial dispositions to the reacting functional groups.[4] The proximity achieved by such noncovalent interactions is considered responsible for the remarkably enhanced rates. Traditionally, chemists have sought to simulate this precompression along a reaction coordinate by examining related intramolecular reactions.[4,5] Although such processes often enjoy kinetic acceleration, their relative rates have been found to vary appreciably. As a consequence, considerable controversy has arisen.[6,7] Page and Jencks have compiled no less than 21 different well-defined attempts to formulate a theory of enzymatic catalysis.[8] Clearly, if intramolecular reactions are to serve as useful approximations of enzymatic processes, paramount attention needs to be given to sorting out the individual factors that contribute to rate acceleration and to according the proper weighting to them.[8,9]

In recent years, dyotropic rearrangements[10] have emerged as notably serviceable probes of proximity effects.[11–17] This is because positional interchanges of atoms in this manner (especially hydrogens) occur intramolecularly in the absence

[⊗] Abstract published in *Advance ACS Abstracts*, November 1, 1994.

(1) BP America Fellow, 1991; National Needs Fellow, 1989–1990; University Fellow, 1988–1989.

(2) Author to whom inquiries relative to the X-ray crystallographic studies should be addressed at the Northern Illinois University address.

(3) (a) Page, M. I. In *The Chemistry of Enzyme Action*; Page, M. I., Ed.; Elsevier: Amsterdam, 1984; pp 1–54. (b) Jencks, W. P. *Adv. Enzymol.* **1975**, *43*, 219. (c) Fersht, A. R. *Enzyme Structure and Mechanism*, 2nd ed.; Freeman: San Francisco, 1984. (d) Page, M. I. In *Enzyme Mechanisms*; Page, M. I., Williams, A., Eds.; Royal Society of Chemistry: London, 1987.

(4) Czarnik, A. W. In *Mechanistic Principles of Enzyme Activity*; Liebman, J. F., Greenberg, A., Eds.; VCH Publishers, Inc.: New York, 1986.

(5) (a) Jencks, W. P. *Catalysis in Chemistry and Enzymology*; McGraw-Hill: New York, 1969. (b) Bruice, T. C.; Benkovic, S. J. *Bio-organic Mechanisms*; W. A. Benjamin: New York, 1966; Vol. 1. (c) Page, M. I. *Chem. Soc. Rev.* **1973**, *2*, 295.

(6) (a) Menger, F. M.; Venkataram, U. V. *J. Am. Chem. Soc.* **1985**, *107*, 4706. (b) Menger, F. M. *Acc. Chem. Res.* **1985**, *18*, 125. (c) Menger, F. M. *Adv. Mol. Model.* **1988**, *1*, 189. (d) Sherrod, M. J.; Menger, F. M. *J. Am. Chem. Soc.* **1989**, *111*, 2611. (e) Menger, F. M.; Sherrod, M. J. *J. Am. Chem. Soc.* **1990**, *112*, 8071. (f) Sherrod, M. J.; Menger, F. M. *Tetrahedron Lett.* **1990**, *31*, 459.

(7) (a) Dorigo, A. E.; Houk, K. N. *J. Am. Chem. Soc.* **1987**, *109*, 3698. (b) Dorigo, A. E.; Houk, K. N. *Adv. Mol. Model.* **1988**, *1*, 135.

(8) Page, M. I.; Jencks, W. P. *Gazz. Chim. Ital.* **1987**, *117*, 455.

(9) Page, M. I. *J. Mol. Catal.* **1988**, *47*, 241.

(10) Reetz, M. T. *Angew. Chem., Int. Ed. Engl.* **1972**, *11*, 129; *Adv. Organomet. Chem.* **1977**, *16*, 33.

(11) (a) Mackenzie, K. *J. Chem. Soc.* **1965**, 4646. (b) Mackenzie, K. *J. Chem. Soc. C* **1969**, 1784. (c) Mackenzie, K.; Adams, C. H. M. *J. Chem. Soc. C* **1969**, 480. (d) Mackenzie, K.; Proctor, G. J.; Woodnut, D. J. *Tetrahedron Lett.* **1984**, *25*, 977. (e) Mackenzie, K.; Proctor, G.; Woodnut, D. J. *Tetrahedron* **1987**, *43*, 5981. (f) Howard, J. A. K.; Mackenzie, K.; Johnson, R. E.; Astin, K. B. *Tetrahedron Lett.* **1989**, *30*, 5005. (g) Mackenzie, K.; Gravett, E. C.; Gregory, R. J.; Howard, J. A. K.; Maher, J. P. *Tetrahedron Lett.* **1992**, *33*, 5629.

(12) (a) Srinivasan, R. *Tetrahedron Lett.* **1973**, 4029. (b) Ginsburg, D. *Tetrahedron* **1974**, *30*, 1487. (c) See also: Sato, K.; Yamashita, Y.; Mukai, T. *Tetrahedron Lett.* **1981**, *22*, 5303. (d) Mulzer, J.; Brüntrup, G. *Angew. Chem., Int. Ed. Engl.* **1979**, *18*, 793.

(13) (a) Black, T. H.; DuBay, W. J., III. *Tetrahedron Lett.* **1987**, *28*, 4787; **1988**, *29*, 1747. (b) Black, T. H.; Hall, J. A.; Sheu, R. G. *J. Org. Chem.* **1988**, *53*, 2371.

(14) (a) Chow, T. J.; Ding, M.-F. *Angew. Chem., Int. Ed. Engl.* **1986**, *25*, 1121. (b) Marchand, A. P.; Annapurna, P.; Watson, W. H.; Nagl, A. *J. Chem. Soc., Chem. Commun.* **1989**, 281.

(15) Hagenbuch, J.-P.; Stampfli, B.; Vogel, P. *J. Am. Chem. Soc.* **1981**, *103*, 3934.

(16) Kluft, E.; Nibbering, N. M. M.; Kühn, H.; Herzschuh, R. *J. Am. Chem. Soc.* **1986**, *108*, 7201.

0002-7863/94/1516-10883$04.50/0

of catalysts and have the latent potential for operating under orbital symmetry control.[18] Various aspects of hydrogen dyotropy have also been accorded intense theoretical scrutiny.[7,19-22] From our vantage point, *syn*-sesquinorbornene disulfones[23] exemplified by **1** were considered to be attractive

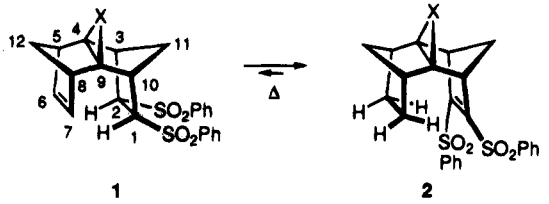

1 **2**

a, X = H, H; **b**, X = O; **c**, X = CH_2

substrates for investigation because molecules of this type promised to be inherently free of many mechanistic assumptions. Furthermore, by the proper manipulation of X, it was considered possible to alter progressively the intracavity distance that separates the reaction centers, to determine the magnitude of these distances by X-ray crystallography, and to correlate the intracavity distance with reaction rate.[24]

Although a superb correlation has been found for these "parent" systems, there remained unanswered those pivotal questions bearing on whether distance was the sole kinetic determinant and whether the translocation of hydrogen occurred concertedly or in a stepwise manner. Herein we show that the impressive rate profile originally seen with **1** is distinctive in other ways not controlled exclusively by distance.[25] By modifying the structural features of **1** to incorporate added ground-state strain, we have found that the intragap compression is not heightened, but that the associated transition-state barriers are nevertheless lowered significantly. There can be no question therefore that proximity is not the sole determinant of rate, although it does play an important role. In the companion paper,[26] primary deuterium isotope effects are reported, theoretical analyses are applied, and quantum tunneling is shown to operate as a significant mechanistic pathway in these systems.

Results and Discussion

Synthesis of the *syn*-Sesquinorbornene Disulfones. In order to achieve different levels of steric compression or long-range homoconjugation[27] not present in **1**, recourse was made to three modes of framework substitution. The first category, consisting of the several derivatives found in Scheme 1, features the positioning of an isopropylidene or spirocyclopropyl group at the apical carbon most proximal to the pair of phenylsulfonyl substituents. Hydrocarbon **3a**, which has been earlier described,[28] is a relatively unreactive Diels–Alder diene. Its conversion to **4a** required that the cycloaddition with (*Z*)-1,2-bis(phenylsulfonyl)ethylene[29] be performed in a high-pressure reactor at 90 000 psi.[28]

Scheme 1

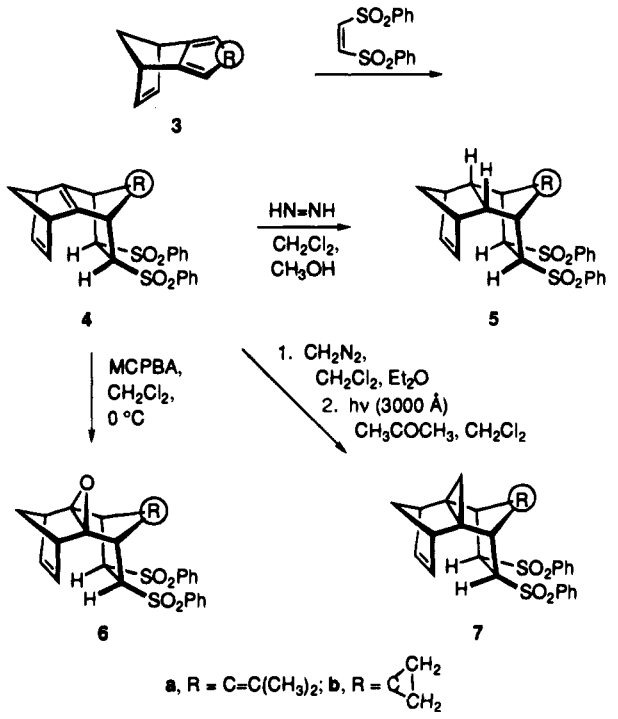

The preparation of **3b** was achieved by reaction of tricyclo-[5.2.1.$0^{2,6}$]deca-2,5,8-triene[30] with excess potassium hydride in the presence of 1,2-dibromoethane as a solute in cold (−40 °C) DMF.[31] Maintaining THF solutions of **3b** and the same dienophile at 25 °C and 160 000 psi for 5 days resulted in efficient conversion (87%) to a 1:1 mixture of **4b** and its endo,endo isomer. Subsequently, the central double bond in adducts **4a** and **4b** was regioselectively reduced with diimide to give **5**, epoxidized with MCPBA to produce **6**, and cyclopropanated in two stages to generate **7**.

The disulfones of the second type were designed to carry the same two groups on the apical carbon positioned above the etheno bridge as in **10**–**12** (Scheme 2). Procedures for the acquisition of **8a** and **9a** had previously been detailed[28] and were consequently followed. To arrive at **9b**, the known 7-spirocyclopropanebicyclo[2.2.1]hept-5-ene-2,3-dione[32] was subjected to 2-fold olefination with the bisWittig reagent available from exposure of 1,3-bis(triphenylphosphonio)propane dibromide to *n*-butyllithium in THF.[33] These conditions provided **8b** in 18% yield, the level of efficiency being in the normal range for this annulation protocol. Like **8a**, **8b** is a reasonably reactive Diels–Alder diene such that simple stirring with an equimolar amount of (*Z*)-1,2-bis(phenylsulfonyl)ethylene at room temperature for 5 days furnished **9b** in 98% yield. The conversion of **9a** and **9b** to **10**–**12** was performed as before.

(17) (a) Geich, H.; Grimme, W.; Proske, K. *J. Am. Chem. Soc.* **1992**, *114*, 1492. (b) Frontera, A.; Suñer, G. A.; Deyà, P. M. *J. Org. Chem.* **1992**, *57*, 6731.
(18) Reetz, M. T. *Tetrahedron* **1973**, *29*, 2189.
(19) Goddard, W. A. *J. Am. Chem. Soc.* **1972**, *94*, 793.
(20) Feller, D. F.; Schmidt, M. W.; Ruedenberg, K. *J. Am. Chem. Soc.* **1982**, *104*, 960.
(21) Jensen, F. *J. Am. Chem. Soc.* **1992**, *114*, 1596.
(22) McKee, M. L.; Stanbury, D. M. *J. Am. Chem. Soc.* **1992**, *114*, 3214.
(23) Paquette, L. A.; Künzer, H.; Green, K. E.; DeLucchi, O.; Licini, G.; Pasquato, L.; Valle, G. *J. Am. Chem. Soc.* **1986**, *108*, 3453.
(24) Paquette, L. A.; Kesselmayer, M. A.; Rogers, R. D. *J. Am. Chem. Soc.* **1990**, *112*, 284.
(25) Paquette, L. A.; O'Doherty, G. A.; Rogers, R. D. *J. Am. Chem. Soc.* **1991**, *113*, 7761.
(26) Houk, K. N.; Li, Y.; McAllister, M. A.; O'Doherty, G. A.; Paquette, L. A.; Siebrand, W.; Smedarchina, Z. K. *J. Am. Chem. Soc.*, following paper in this issue.
(27) Paquette, L. A; Waykole, L.; Shen, C.-C.; Racherla, U. S.; Gleiter, R.; Litterst, E. *Tetrahedron Lett.* **1988**, *29*, 4213.
(28) (a) Paquette, L. A.; Shen, C.-C. *Tetrahedron Lett.* **1988**, *29*, 4069. (b) Paquette, L. A.; Shen, C.-C.; Engel, P. *J. Org. Chem.* **1989**, *54*, 3329.
(29) DeLucchi, O.; Lucchini, V.; Pasquato, L.; Modena, G. *J. Org. Chem.* **1984**, *49*, 596.
(30) Böhm, M. C.; Carr, R. V. C.; Gleiter, R.; Paquette, L. A. *J. Am. Chem. Soc.* **1980**, *102*, 7218.
(31) Paquette, L. A.; Charumilind, P.; Böhm, M. C.; Gleiter, R.; Bass, L. S.; Clardy, J. *J. Am. Chem. Soc.* **1983**, *105*, 3136.
(32) (a) Scharf, H.-D.; Liebig, D. *Angew. Chem., Int. Ed. Engl.* **1968**, *7*, 215. (b) Blankespoor, R. L.; Gollehon, D. *J. Org. Chem.* **1977**, *42*, 63.
(33) (a) Burgstahler, A. W.; Boger, D. L.; Naik, N. C. *Tetrahedron* **1976**, *32*, 309. (b) Paquette, L. A.; Green, K. E.; Gleiter, R.; Schäfer, W.; Gallucci, J. C. *J. Am. Chem. Soc.* **1984**, *106*, 8232.

Scheme 2

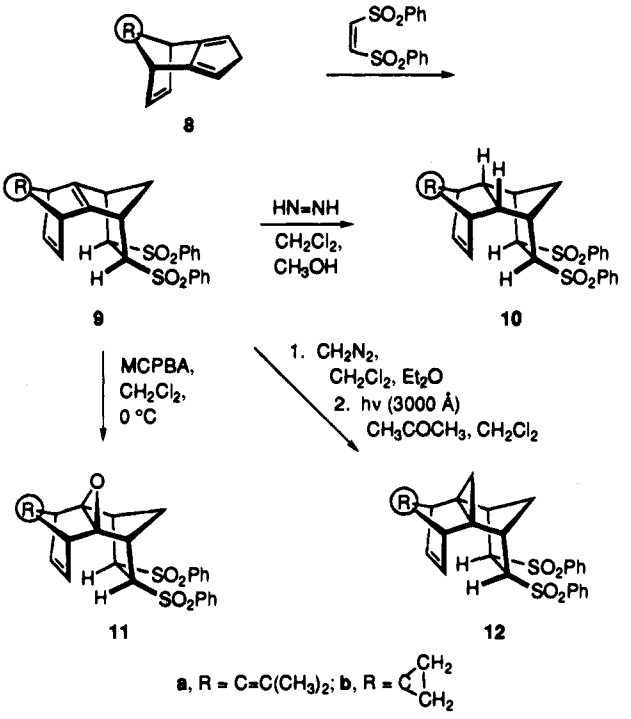

Scheme 3

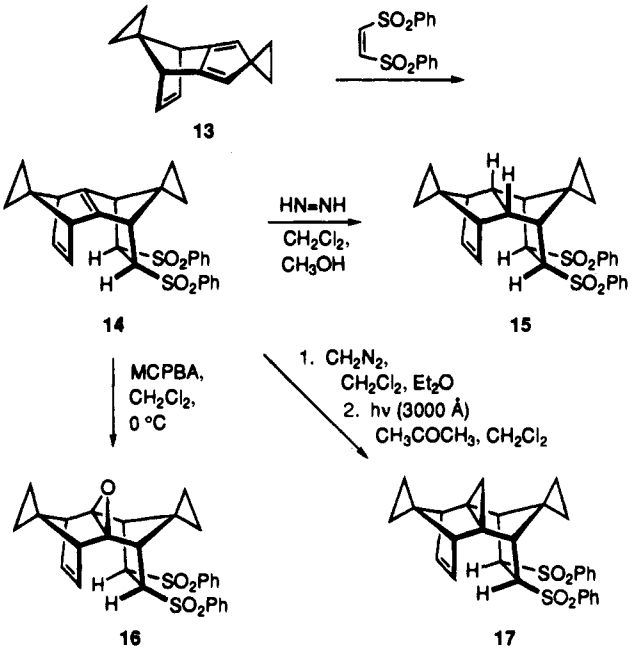

Spirocyclopropanation of **8b** gave rise to **13** and subsequently **14** (Scheme 3). This adduct and its functionalized derivatives **15**–**17** are seen to be sterically crowded at both apical sites.

Molecular Structure Studies. The precise molecular geometries of all 15 compounds whose kinetic responses were to be quantified were obtained by X-ray crystallographic methods as shown in Figures 1–3. These ORTEP drawings, pictured with 50% probability ellipsoids, have the phenyl groups omitted so as to achieve added clarity. All of the crystallographic data has been included in the supplementary material except for the generically defined nonbonded distances C(1)-H–C(7) and C(2)-H–C(6), and the intracavity angles (C(7)–H-(C1) and C(6)–H-(C2)). Inspection of Figures 1–3 and Table I reveals that, like **2a-2c**,[24] many of the disulfones are slightly twisted in the crystalline state such that the two distances of direct interest are modestly different. In order to achieve some simplification in the plotting of data, the two nonbonded distances have been averaged. However, the unequal gaps hold significance that will be discussed in the sequel.[26]

Direct comparison of the molecular structures is facilitated by compartmentalizing the disulfones according to the type of central substitution. As concerns the dihydro series, **5a** and **10b** exhibit the closest average intragap distance of 2.36 Å. However, the intracavity angles for this pair of compounds are rather different, the mismatch on both corners being among the largest observed throughout the series (Table 1). At 2.41 Å, the average nonbonded C(1)-H–C(7) and C(2)-H–C(6) distances for **1a** and **5b** are seen to be 0.05 Å larger than above. In this case, the associated intracavity angles are relatively comparable at 117.9–123.8°. On the basis of intraannular gap considerations alone, **1a** and **5b** clearly occupy a position central between the somewhat more compressed **5a** and **10b** and the less crowded **10a** (2.48 Å) and **15** (2.47 Å). Should proximity factors contribute *uniquely* to the rate of thermal isomerization of these six compounds, the relative ordering should fall in the order **5a** > **10b** > **1a** > **5b** > **15** ~ **10a**.

The experimentally determined geometric features of the epoxides differ significantly from those found in the diimide products. Thus, the effect of positioning an apical cyclopropyl group as in **6b** is to minimize the intracavity distance the most (2.34 Å). The gap spread in this series is the largest observed (2.34–2.53 Å), with **1b** and **11a** exhibiting the lowest levels of steric compression. On this basis alone, the relative reactivity of these systems would be expected to be **6b** > **16** > **6a** > **11b** > **11a** > **1b**. The associated intracavity angles are similarly distinctive in the degree to which they are altered (Table 1).

One major consequence of central double bond cyclopropanation is a reduction in the magnitude of the intracavity gaps. The effect is in a direction opposite to that observed in the epoxide series principally because the newly introduced CH_2 groups carry two hydrogen atoms that must be sterically accommodated. The differing C–O bond lengths and angles within the oxirane ring could, of course, also be contributory. The global consequences of these combined effects surface in the form of minimal structural differences between the several cyclopropanated disulfones (Table 1) relative to their dihydro and epoxy counterparts. Notwithstanding, it remains possible to assign a *compression-based* reactivity order, viz. **7b** > **17** > **1c** > **12b** > **7a** > **12a**, as long as experimental artifacts or crystal packing effects are absent or of no consequence.

For obvious reasons, acquisition of the intermediate pyrazoline **18** in crystalline form prompted an X-ray crystallographic determination of its structure. A comparison between **16**, **17**,

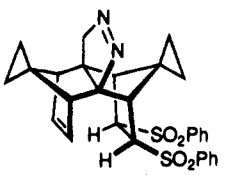

18

and **18** was anticipated to provide some insight into the extent to which the basic *syn*-sesquinorbornene framework of these closely related congeners would be deformed by the nature and spatial demands of the central ring. The heterocycle **18** crystallized with two different molecules in the asymmetric unit (see Figure 4 for the ORTEP diagram of molecule A). The C(1)-H–C(7) and C(2)-H–C(6) distances were determined to be 2.38 and 2.42 Å, respectively, in molecule A, and 2.22 and 2.47 Å in molecule B. Although B is rather more twisted than

A, the averaged distance (2.37 Å) positions **18** between **16** and **17**. All three are more compressed than **15**. Consequently, the molecular scaffolding that characterizes these systems appears to respond with reasonable predictability to nonbonded steric compression in those various sectors where it is present.

Product Studies. The capacity of all the disulfones (exclusive of **18**) for dyotropic rearrangement was initially assessed by heating the individual samples in bromobenzene. In order to accommodate the differing levels of reactivity noted in pilot experiments, the preparative scale runs were performed either at 100 °C (for **7b** and **17**), 120 °C (for **5a**, **5b**, **7a**, **10b**, **12b**, and **15**), or 160 °C (for **6a**, **6b**, **11a**, **11b**, and **16**). Reaction times ranged from 24 to 48 h as indicated in the Experimental Section. Partial decomposition was noted during the isomerization of **11a**, such that the yield of isolated **23a** did not surpass the 25% level. The cyclopropanated disulfone **12a** unexpectedly proved to be thermally labile and decomposed during attempts to effect its conversion to **24a**. Consequently, **24a** was never acquired or characterized. Otherwise, the conversions to the respective enedisulfones **19**–**27** proceeded smoothly. Successful operation of each rearrangement was convincingly diagnosed by the disappearance of the olefinic (δ 6.5–6.0) and α-sulfonyl proton absorptions (δ 4.0–3.6) in favor of a two-proton multiplet at higher field. The increased shielding accompanying the loss of allylic character to the bridgehead protons in the non-sulfur-substituted norbornyl ring proved to be similarly diagnostic.

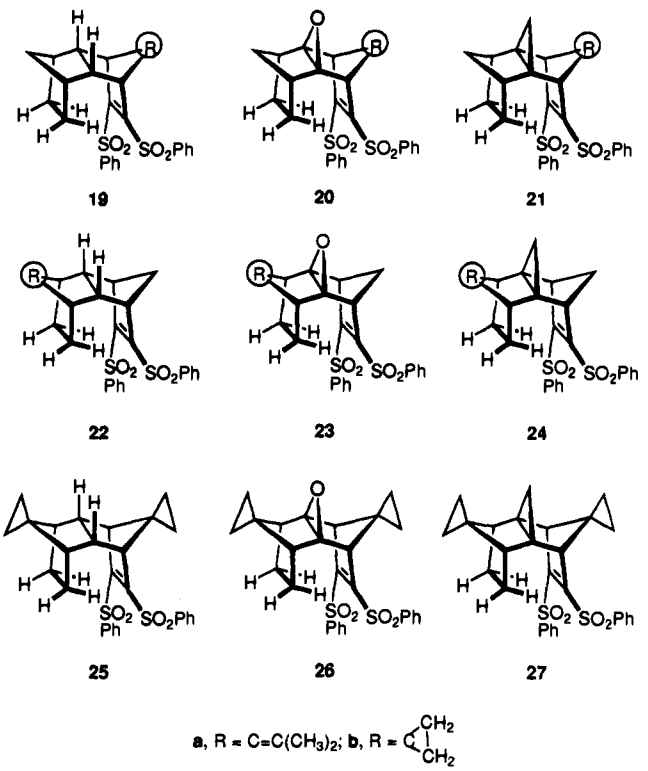

Kinetic Measurements. The absolute rate constants compiled in Table 2 were determined in C_6D_5Br solution by suitable monitoring of key spectral changes by ^1H NMR spectroscopy at 300 MHz. Although the appreciable temperature range required for the proper acquisition of these data necessitated the adaptation of two somewhat different laboratory procedures, three disulfones (**7b**, **12b**, and **17**) examined under both sets of conditions were found to give kinetic profiles that were identical within experimental error.

In generic terms, the epoxy disulfones constitute the least reactive subgroup examined in this study. Conversely, the presence of a central cyclopropane ring exerts a notable accelerating effect on the dyotropic change. The result of plotting the log k_{rel} values for the 16 compounds listed in Table 2 against the average $PhSO_2C$-H–sp^2-C distances is seen in Figure 5. Although the absence of a good correlation is clear (r = 0.83), key departures from linearity are disguised by presentation of the data in this fashion. The most significant of these is made apparent when the kinetic behavior of the dihydro disulfones is analyzed separately (Figure 6). For this series, the experimentally-determined reactivity order of **15** > **10b** > **5a** > **10a** > **5b** > **1a** correlates extremely poorly (r = 0.33) with the differences in magnitude of the intracavity gap.

Instead, the relative rearrangement rates give evidence of adhering to a trend having its origins in the steric interactions present in four other zones within these disulfones (see **28**).

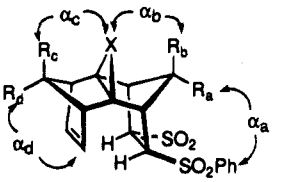

28

These are defined as α_a, the compression existent between R_a and the two sulfone subunits; α_b, the nonbonded steric interaction between R_b and the group X; α_c, a very similar R_c-X strain factor; and α_d, the structurally enforced proximity of R_d to the norbornenyl double bond. Ground-state destabilization can in principle be achieved at any of the four sites, especially by positioning a cyclopropane ring there. Further exacerbation of the situation materializes when X is similarly constituted.

The kinetic ordering among the dihydro disulfones suggests that the ground-state strain in **15** is sufficiently elevated that this compound experiences the least difficulty in passing over the transition state barrier associated with the intramolecular dyotropic shift. Compound **10a**, which features an intracavity gap entirely comparable to that present in **15**, is more than 4 times less reactive. This dropoff in rate can seemingly be attributed to the considerable dimunition of steric congestion in the α_c and α_d zones.

The epoxide correlation (Figure 7) is also subpar (r = 0.65). In this subset, the enhanced reactivity of **16** can be similarly attributed to steric compression in all four zones. Although the $PhSO_2C$-H–sp^2-C distance in **6b** is reduced by nearly 0.1 Å relative to **16**, the rate of rearrangement of **6b** is roughly half that of its biscyclopropane homolog. Thus, although the oxygen atom at X is well-separated from the reaction site, its role in controlling rate is not governed completely by the distance necessarily traversed by the hydrogens undergoing translocation.

Very similar trends govern the rates of the most reactive cyclopropanated disulfones (Figure 8, r = 0.83). Despite the fact that the intracavity gaps for **1c** and **17** differ by only 0.02 Å, a 25-fold rate acceleration favoring tricyclopropane **17** is to be noted.

Additional insight into the nature of the principal rate-controlling factor can be derived from other comparisons. For example, the presence of an apical cyclopropane ring proximal to the two phenylsulfonyl groups uniformly enhances reaction rate relative to those isomeric systems that carry the apical cyclopropane in the "remote" norbornene subunit. This trend, while not always accompanied by increased compression across the intracavity gap, is characterized, however, by larger values of K_{eq} in the first subset: **5b** (2.41 Å), k_{rel} = 116, K_{eq} = 30 versus **10b** (2.36 Å), k_{rel} = 42, K_{eq} = 3; **6b** (2.34 Å), k_{rel} = 16,

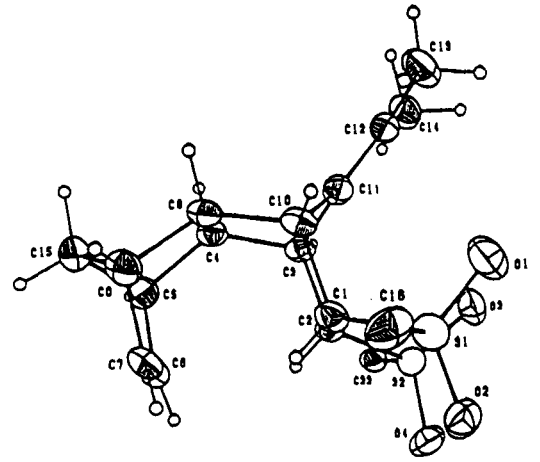

5a

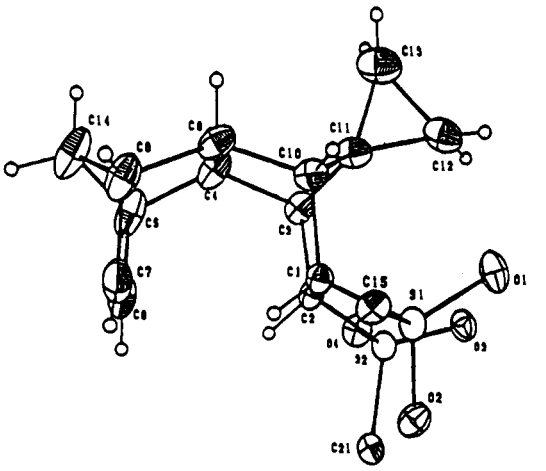

5b

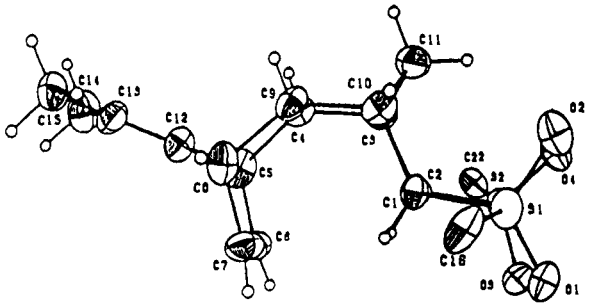

10a

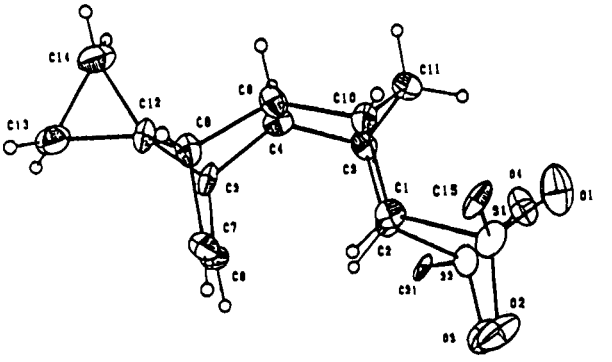

10b

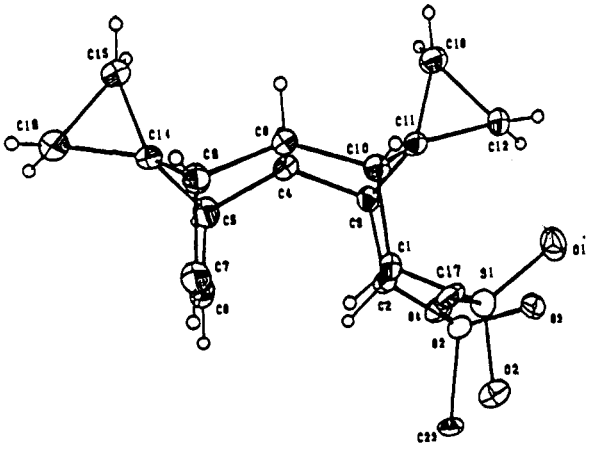

15

Figure 1. Structures of the dihydro *syn*-sesquinorbornene disulfones.

K_{eq} = 10 versus **11b** (2.47 Å), k_{rel} = 14, K_{eq} = 3; **7b** (2.25 Å), k_{rel} = 6700, K_{eq} = 60 versus **12b** (2.33 Å), k_{rel} = 939, K_{eq} = 9.

More impressive yet are the consequences of progressing from **5b-7b** to those homologues that carry two apical cyclopropanes, viz. **15**–**17**. In all three series, spiroalkylation of the apical carbons in this manner serves to increase concurrently the distance across the intracavity gap, k_{rel}, and K_{eq} (see Table 1). *These results clearly contraindicate the view that intramolecular dyotropic reactions are controlled exclusively by distance.*

The orientation of functional groups appropriate for ensuing chemical reaction is a necessary prelude to chemical change. For *syn*-sesquinorbornenes of the type examined here, the small $\Delta S^{\ddagger}$ values indicate that the changes in freedom of motion that occur while progressing to the transition states for hydrogen diotropy do not contribute in a dominant way to reaction rate. Consequently, other influences that provide greater impact as these rearrangements proceed need to be identified. One key factor that we have identified is associated with the dissimilarities in ground-state strain that gain importance in reducing the energy barrier to various degrees. As always, the reactivity determinant in this series is the energy difference separating the specific ground state molecule from its dyotropic transition

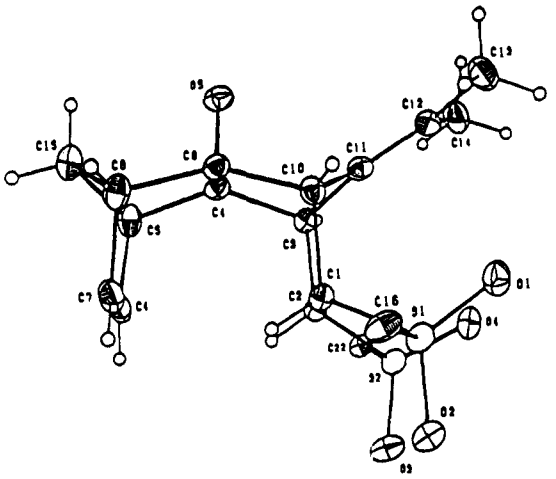

6a

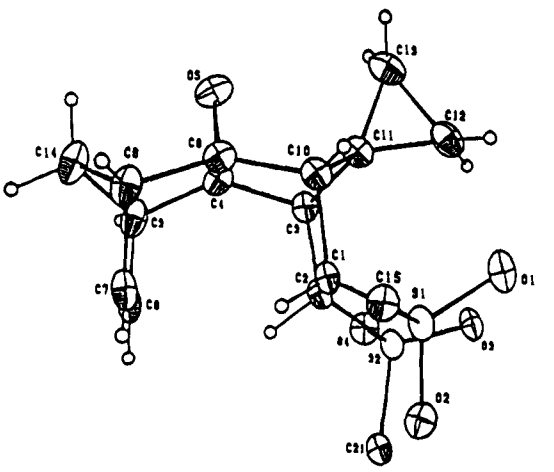

6b

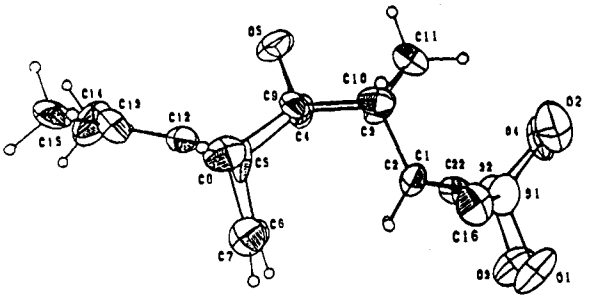

11a

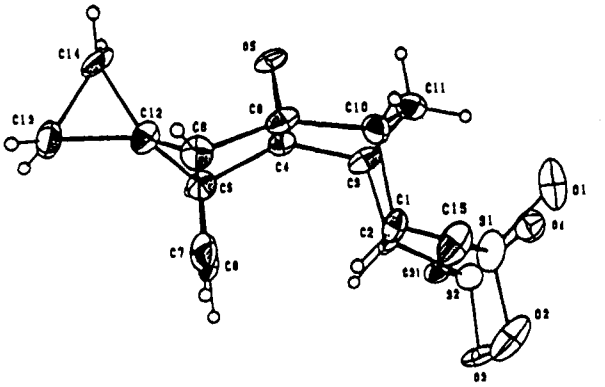

11b

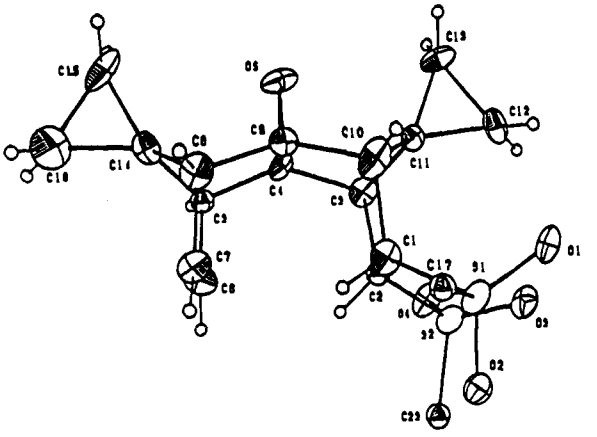

16

Figure 2. Structures of the *syn*-sesquinorbornene disulfone epoxides.

state. This process gives every indication of being made less costly by the introduction of nonbonded steric compression into the $\alpha_a-\alpha_d$ zones rather than added compression within the intracavity gap.

Unanswered by the present investigation is whether the α-sulfonyl hydrogens migrate concertedly in $\sigma_{2s} + \sigma_{2s} + \pi_{2s}$ fashion or do so stepwise via a tunneling mechanism that would effectively skirt the full energetic costs associated with the formation of biradical intermediates. These issues are addressed in the paper that follows.[26]

Experimental Section

Melting points are uncorrected. Infrared spectra were recorded on a Perkin-Elmer Model 1320 spectrometer. ^{1}H NMR spectra were recorded at 300 MHz and the ^{13}C NMR data obtained by 75, 62.5, 50, or 20 MHz as indicated. Mass spectra were measured on a Kratos MS-30 instrument at The Ohio State University Campus Chemical Instrumentation Center. Elemental analyses were performed at the Scandinavian Microanalytical Laboratory, Herlev, Denmark. All flash chromatographic separations were carried out on Merck silica gel 60 (60–200 mesh), and reactions (exclusive of the high pressure processes)

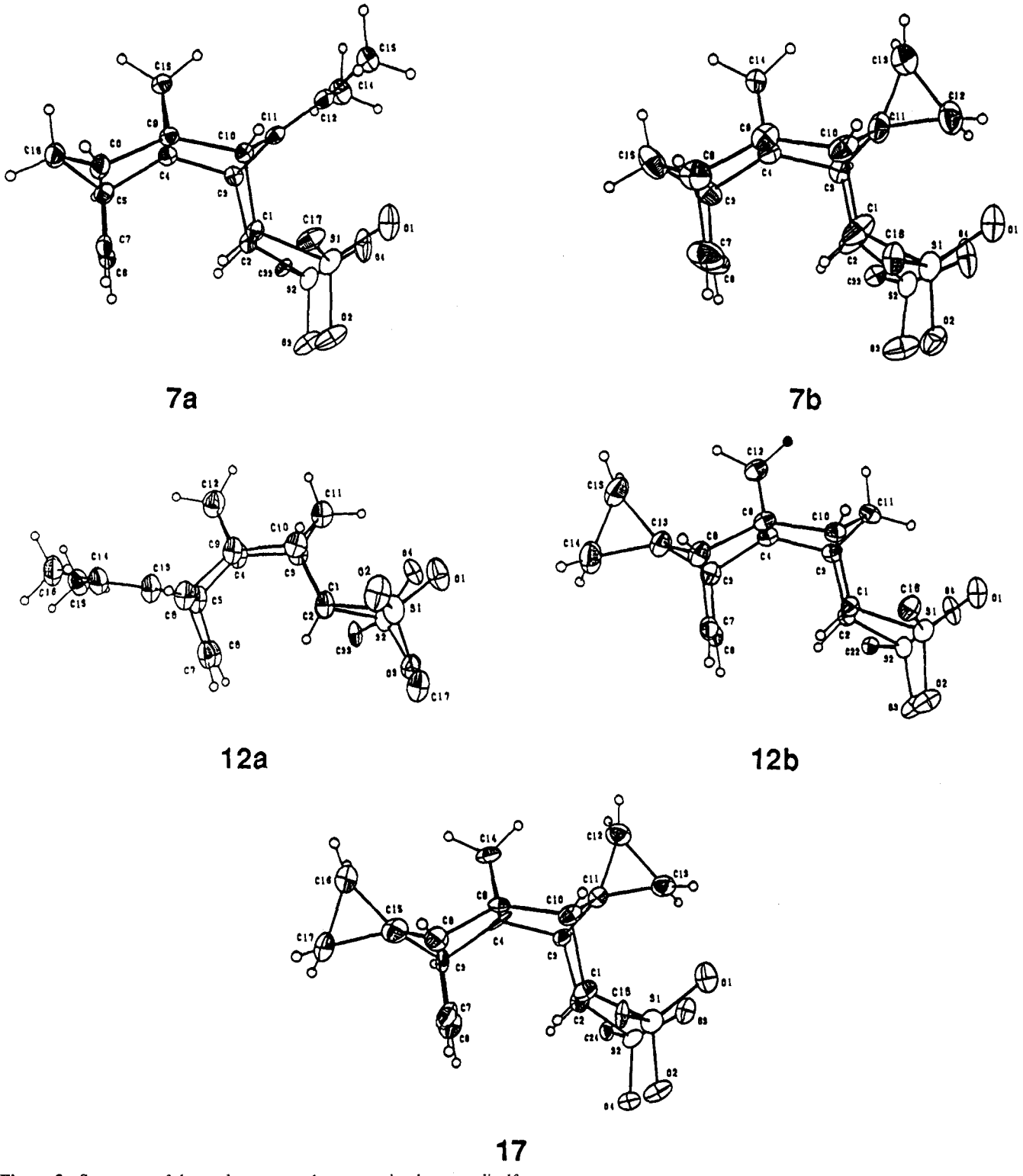

Figure 3. Structures of the cyclopropanated *syn*-sesquinorbornene disulfones.

were routinely performed under an inert atmosphere unless otherwise indicated. Solvents were reagent grade and dried prior to use.

Preparation of the Functionalized Tricyclo[5.2.1.0^{2,6}]deca-2,5,8-trienes. The trienes **3a**,[28] **8a**,[28] and **8b**[28] have been earlier described. The spirocyclopropanations leading to **3b** and **13** were performed as follows. To a suspension of KH (3.3 g, 80 mmol) in dry DMF (200 mL) cooled to −45 °C was introduced a solution of tricyclo[5.2.1.0^{2,6}]-deca-2,5,8-triene[30] (3.0 g, 23 mmol) in anhydrous THF (25 mL) by syringe. After 30 min of stirring,1,2-dibromoethane was slowly added, the mixture was stirred overnight at room temperature, and water (200 mL) was carefully dropped in. The product was extracted with pentane (5 × 100 mL), and the combined organic layers were washed with 10% HCl (200 mL) and brine (100 mL) prior to drying and solvent evaporation. The residue was chromatographed on silica gel (pentane elution) to give 980 mg (28%) of **3b** as a clear oil: IR (neat, cm^{-1}) 2960, 2920, 2870, 1395, 1210, 1105; ^{1}H NMR (300 MHz, $CDCl_3$) δ 6.46 (dd, J = 1.5, 1.5 Hz, 2 H), 5.42 (s, 2 H), 3.57 (s, 2 H), 2.31 (dt, J = 7.8, 1.5 Hz, 1 H), 2.12 (d, J = 7.8 Hz, 1 H), 1.30−0.88 (m, 6 H); ^{13}C NMR (75 MHz, $CDCl_3$) ppm 151.5, 138.9, 121.9, 59.7, 43.9, 41.0, 11.0, 10.8; MS m/z (M^+) calcd 156.3474, obsd 156.3475.

7-Spirocyclopropane bicyclo[2.2.1]hept-5-ene-2,3-dione[32] (1.00 g, 6.6 mmol) was added slowly to a solution of bis-Wittig reagent, prepared by stirring 1,3-bis(triphenylphosphonio)propane dibromide (4.80 g) and 8.8 mL of 1.5 M n-butyllithium in 50 mL of THF overnight. The reaction mixture was stirred for 2 h at room temperature and at 45 °C for 3 days, then extracted with water and pentane. The

Table 1. Relevant Experimentally Determined Structural Parameters (X-ray Methods)

	nonbonded distances, Å			intracavity angles, deg	
compd	C(1)–H–C(7)	C(2)–H–C(6)	average distance	C(7)–H–C(1)	C(6)–H–C(2)
		A. Dihydro Disulfones			
1a	2.44	2.37	2.41	117.9	122.0
5a	2.36	2.36	2.36	127.6	128.5
5b	2.38	2.43	2.41	123.8	120.5
10a[a]	2.42	2.52	2.48[b]	123.9	119.3
	2.43	2.54		122.5	118.4
10b[a]	2.37	2.37	2.36[b]	121.5	118.8
	2.37	2.34		119.3	124.4
15	2.44	2.49	2.47	122.7	120.3
		B. Epoxy Disulfones			
1b	2.60	2.46	2.53	117.3	123.1
6a	2.43	2.47	2.45	126.2	127.5
6b	2.37	2.31	2.34	131.7	128.2
11a	2.54	2.49	2.52	117.9	121.1
11b	2.42	2.53	2.47	124.1	119.5
16	2.38	2.47	2.43	127.8	117.9
		C. Cyclopropanated Disulfones			
1c	2.32	2.31	2.32	121.2	122.4
7a	2.30	2.39	2.35	125.4	120.8
7b	2.27	2.23	2.25	126.3	129.6
12a	2.40	2.33	2.37	121.0	124.7
12b	2.35	2.31	2.33	122.7	123.2
17	2.33	2.27	2.30	124.5	128.5

[a] These compounds contain two different molecules in the asymmetric unit. [b] Average of all four data points.

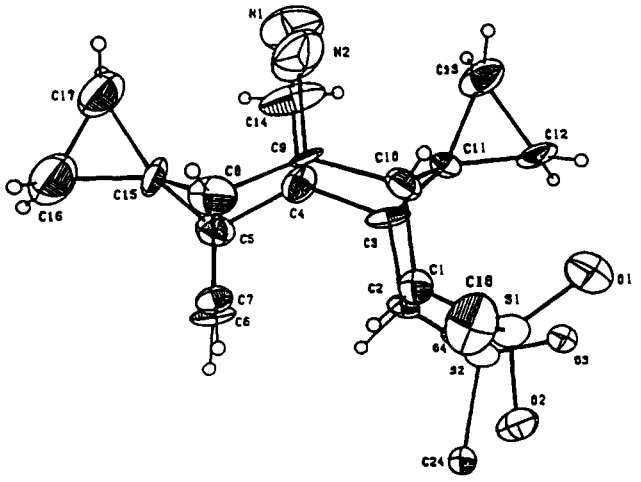

Figure 4. Structure of the diazomethane adduct 18.

organic phase was dried and evaporated, and the residue was chromatographed on silica gel (pentane elution) to give 195 mg (19%) of **8b** as a colorless solid: mp 45–50 °C; IR (neat, cm^{-1}) 2960, 2920, 2870, 1395, 1210, 1105; ^1H NMR (300 MHz, $CDCl_3$) δ 6.43 (dd, J = 1.8, 1.8 Hz, 2 H), 5.67 (s, 2 H), 3.30 (t, J = 1.5 Hz, 2 H), 2.85 (s, 2 H), 0.70–0.60 (m, 2 H), 0.60–0.50 (m, 2 H); ^{13}C NMR (75 MHz, $CDCl_3$) ppm 153.9, 137.7, 114.0, 54.2, 49.7, 46.2, 8.3, 7.2; MS *m/z* (M^+) calcd 156.0938, obsd 156.0938.

The spirocyclopropanation of **8b** (500 mg, 2.75 mmol) in a manner paralleling that described above furnished 150 mg (30%) of **13** as a colorless oil: IR (neat, cm^{-1}) 2960, 2920, 2870, 1395, 1210, 1105; ^1H NMR (300 MHz, $CDCl_3$) δ 6.52 (dd, J = 1.8, 1.8 Hz, 2 H), 5.39 (s, 2 H), 2.91 (s, 2 H), 1.10–0.80 (m, 4 H), 0.68–0.50 (m, 4 H); ^{13}C NMR (75 MHz, $CDCl_3$) ppm 150.9, 138.4, 121.4, 54.6, 50.1, 40.6, 11.2, 10.8, 8.6, 7.3; MS *m/z* (M^+) calcd 182.1095, obsd 182.1010.

Preparation of the *syn*-Sesquinorbornene Disulfones. General Procedure. Fulvene **3a** (1.0 g, 5.96 mmol) and (*Z*)-1,2-bis(phenylsulfonyl)ethylene[29] (1.90 g, 6.0 mmol) were dissolved in CH_2Cl_2 or THF (5 mL, deoxygenated), sealed inside a Teflon tube, and subjected to 160 000 psi in a high-pressure reactor for 5 days. A white precipitate was filtered off before hexane was added to induce further precipitation.

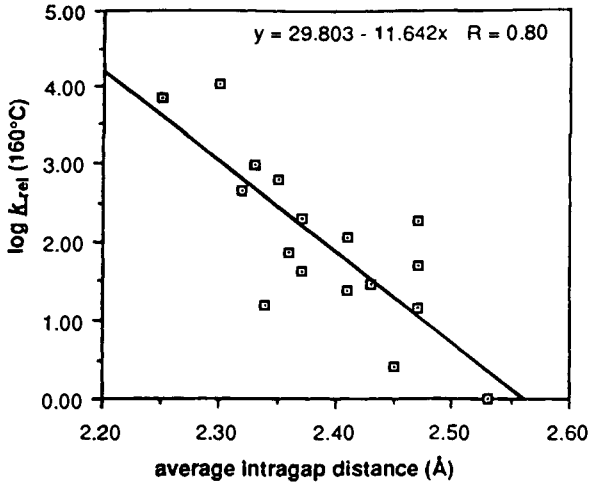

Figure 5. Plot of log k_{rel} (160 °C) versus the average intragap distance (A) for all compounds.

There was isolated a total of 2.84 g (98%) of **4a** as a white solid mp 180 °C dec, which was stored under argon: IR (film, cm^{-1}) 1445, 1325, 1155, 1085; ^1H NMR (300 MHz, $CDCl_3$) δ 8.00–7.53 (m, 10 H), 6.47 (s, 2 H), 3.86 (s, 2 H), 3.23 (s, 2 H), 2.74 (s, 2 H), 2.04 (d, J = 6.6 Hz, 1 H), 1.87 (d, J = 6.5 Hz, 1 H), 1.79 (s, 6 H); ^{13}C NMR (75 MHz, $CDCl_3$) ppm 159.5, 141.3, 139.2, 138.7, 133.3, 128.9, 128.1, 119.2, 76.6, 69.7, 62.9, 48.6, 47.4; MS molecular ion too fleeting to be accurately mass measured.

For **4b**: From 300 mg (1.90 mmol) of **3b**, 160 000 psi, 5 days; 800 mg (87%) of a 1:1 mixture of isomeric adducts, which were separated by MPLC on silica gel. From 100 mg of the mixture, 45 mg of **4b** could be isolated as a white solid: mp 200 °C dec; IR (film, cm^{-1}) 1445, 1325, 1155, 1085; ^1H NMR (300 MHz, $CDCl_3$) δ 7.93–7.50 (m, 10 H), 6.43 (dd, J = 1.7, 1.7 Hz, 2 H), 3.22 (s, 2 H), 3.04 (s, 2 H), 2.78 (s, 2 H), 2.12 (d, J = 6.6 Hz, 1 H), 1.97 (d, J = 6.6 Hz, 1 H), 1.35 (t, J = 6.7 Hz, 2 H), 0.49 (t, J = 8.1 Hz, 2 H); ^{13}C NMR (75 MHz, $CDCl_3$) ppm 160.2, 141.8, 138.8, 133.3, 128.9, 128.3, 70.2, 65.0, 52.6, 48.5, 41.4, 10.1, 4.4; MS molecular ion too fleeting to be accurately mass measured.

For **9a**: From 300 mg (1.8 mmol) of **8a**, room temperature, 5 days; 850 mg (100%) of **9a**, white solid, mp 120–125 °C dec; IR (film, cm^{-1}) 1445, 1325, 1155, 1085; ^1H NMR (300 MHz, $CDCl_3$) δ 8.00–7.53 (m, 10 H), 6.62 (dd, J =1.8, 1.8 Hz, 2 H), 3.75 (d, J = 1.6 Hz, 2 H), 3.37 (s, 2 H), 2.75 (d, J =1.8 Hz, 2 H), 2.61 (d, J = 9.9 Hz, 1 H), 1.64 (d, J = 8.4 Hz, 1 H), 1.40 (s, 6 H);^{13}C NMR (75 MHz, $CDCl_3$) ppm 159.80, 159.76, 140.8, 139.2, 133.6, 129.0, 128.3, 99.8, 64.1, 48.8, 47.1, 43.4, 18.8; MS molecular ion too fleeting to be accurately mass measured.

For **9b**: From 520 mg (3.33 mmol) of **8b**, room temperature, 5 days; 1.50 g (98%) of **9b**, white solid, mp 235 °C dec; IR (film, cm^{-1}) 1440, 1330, 1150; ^1H NMR (300 MHz, $CDCl_3$) δ 8.03–7.50 (m, 10 H), 6.56 (dd, J = 1.7, 1.7 Hz, 2 H), 3.36 (s, 2 H), 2.79 (d, J = 1.8 Hz, 2 H), 2.67 (s, 2 H), 2.61 (d, J = 9.8 Hz, 1 H), 1.67 (d, J = 9.8 Hz, 1 H), 0.47 (m, 4 H); ^{13}C NMR (75 MHz, $CDCl_3$) ppm 160.6, 140.9, 138.9, 133.5, 128.9, 128.3, 65.9, 64.1, 53.8, 47.1, 43.6, 10.0, 8.0; MS molecular ion was too fleeting to be accurately mass measured.

For **14**: From 150 mg (0.82 mol) of **13**, 160 000 psi, 5 days; 400 mg (100%) of **14**, white solid, mp 175–180 °C dec; IR (film, cm^{-1}) 1445, 1335, 1130, 1080; ^1H NMR (300 MHz, $CDCl_3$) δ 8.20–7.40 (m, 10 H), 6.58 (dd, J = 1.8, 1.8 Hz, 2 H), 3.10 (s, 2 H), 2.85 (s, 2 H), 2.65 (s, 2 H), 1.37 (t, J = 8.1 Hz, 2 H), 0.80–0.30 (m, 6 H); ^{13}C NMR (75 MHz, $CDCl_3$) ppm 159.6, 141.8, 138.8, 133.2, 128.8, 128.2, 65.4, 54.1, 53.4, 52.7, 41.0, 10.1, 10.0, 7.9, 4.4; MS molecular ion too fleeting to be accurately mass measured.

General Procedure for Diimide Reductions. To a cold (0 °C), magnetically stirred solution of **4b** (278 mg, 0.60 mmol) and dipotassium azodicarboxylate (114 mg, 60 mmol) in methanol (25 mL) and CH_2Cl_2 (5 mL) was slowly added acetic acid (1 mL) dissolved in methanol (15 mL) over a 2-h period. The reaction mixture was stirred for 8 h and partitioned between CH_2Cl_2 and water. The organic phase was dried and evaporated, and the residue was purified by silica gel

Table 2. Absolute and Relative Rate Data, Equilibrium Constants, log A, and E_a Values for the Dyotropic Rearrangements

compd	T, °C	k, s^{-1}	K_{eq}	log A	E_a	k_{rel} (160 °C)	compd	T, °C	k, s^{-1}	K_{eq}	log A	E_a	k_{rel} (160 °C)
						A. Dihydro Disulfones							
1a[a]	130	$(4.43 \pm 0.44) \times 10^{-6}$	1.7			24	**10b**	120	$(2.37 \pm 0.24) \times 10^{-5}$	3	11.8	29.5	42
	160	$(4.25 \pm 0.43) \times 10^{-4}$	1.8						$(2.49 \pm 0.24) \times 10^{-5}$				
5a	100	$(6.36 \pm 0.64) \times 10^{-6}$	4	11.7	28.8	72		150	$(3.59 \pm 0.36) \times 10^{-4}$	3			
		$(6.40 \pm 0.64) \times 10^{-6}$							$(3.51 \pm 0.36) \times 10^{-4}$				
	120	$(4.35 \pm 0.5) \times 10^{-5}$	6				**15**	80	$(2.20 \pm 0.22) \times 10^{-6}$	60	11.6	27.9	180
		$(3.90 \pm 0.5) \times 10^{-5}$							$(2.21 \pm 0.22) \times 10^{-6}$				
	150	$(6.67 \pm 0.65) \times 10^{-4}$	8					113	$(6.49 \pm 0.65) \times 10^{-5}$	30			
		$(6.23 \pm 0.65) \times 10^{-4}$							$(6.54 \pm 0.65) \times 10^{-5}$	30			
5b	100	$(1.81 \pm 0.18) \times 10^{-4}$	30	10.2	25.5	116		120	$(1.20 \pm 0.13) \times 10^{-4}$	30			
		$(1.72 \pm 0.18) \times 10^{-4}$							$(1.30 \pm 0.13) \times 10^{-4}$				
	120	$(1.07 \pm 0.10) \times 10^{-3}$	30										
		$(1.05 \pm 0.10) \times 10^{-3}$											
10a	120	$(2.77 \pm 0.27) \times 10^{-5}$	2	12.1	30	49							
		$(2.60 \pm 0.27) \times 10^{-5}$											
	150	$(4.08 \pm 0.41) \times 10^{-4}$	2										
		$(4.00 \pm 0.41) \times 10^{-4}$											
						B. Epoxy Disulfones							
1b[a]	160	$(1.80 \pm 0.18) \times 10^{-5}$				1	**11b**	120	$(6.92 \pm 0.70) \times 10^{-6}$	2	12.2	31.3	14
6a	120	$(1.19 \pm 0.12) \times 10^{-6}$	40	11.7	31.3	2.5			$(6.68 \pm 0.70) \times 10^{-6}$				
		$(1.18 \pm 0.12) \times 10^{-6}$						130	$(1.82 \pm 0.18) \times 10^{-5}$	3			
	130	$(2.68 \pm 0.27) \times 10^{-6}$	30						$(1.68 \pm 0.18) \times 10^{-5}$				
		$(2.64 \pm 0.27) \times 10^{-6}$					**16**	100	$(2.20 \pm 0.22) \times 10^{-6}$	100	11.4	29.2	28
	150	$(2.04 \pm 0.20) \times 10^{-4}$	30						$(2.16 \pm 0.22) \times 10^{-6}$				
		$(2.03 \pm 0.20) \times 10^{-4}$						120	$(1.55 \pm 0.15) \times 10^{-5}$	100			
6b	135	$(3.05 \pm 0.31) \times 10^{-5}$	10	11.6	29.8	16			$(1.53 \pm 0.15) \times 10^{-5}$				
		$(3.10 \pm 0.31) \times 10^{-5}$						150	$(2.50 \pm 0.24) \times 10^{-4}$	100			
	156	$(2.22 \pm 0.22) \times 10^{-4}$	10						$(2.27 \pm 0.24) \times 10^{-4}$				
		$(2.10 \pm 0.22) \times 10^{-4}$											
						C. Cyclopropanated Disulfones							
1c	110	$(1.50 \pm 0.06) \times 10^{-4}$	2.5	11.6	27.2	450	**12b**	80	$(1.45 \pm 0.13) \times 10^{-5}$	10	11.6	25.4	939
		$(1.52 \pm 0.06) \times 10^{-4}$							$(1.45 \pm 0.13) \times 10^{-5}$				
	120	$(3.23 \pm 0.30) \times 10^{-4}$	2.8					126	$(8.20 \pm 0.80) \times 10^{-4}$	8			
		$(2.90 \pm 0.30) \times 10^{-4}$							$(7.50 \pm 0.80) \times 10^{-4}$				
	130	$(7.38 \pm 0.35) \times 10^{-4}$	3.0				**17**	50	$(1.39 \pm 0.14) \times 10^{-5}$	200	11.4	24.4	11,000
		$(6.48 \pm 0.35) \times 10^{-4}$							$(1.39 \pm 0.14) \times 10^{-5}$				
7a	80	$(8.11 \pm 0.83) \times 10^{-6}$	40	11.9	27.2	622		81	$(2.71 \pm 0.30) \times 10^{-4}$	200			
		$(8.54 \pm 0.83) \times 10^{-6}$							$(2.69 \pm 0.30) \times 10^{-4}$				
	113	$(2.11 \pm 0.23) \times 10^{-4}$	30					91	$(1.02 \pm 0.10) \times 10^{-3}$	200			
		$(2.47 \pm 0.23) \times 10^{-4}$							$(1.03 \pm 0.10) \times 10^{-3}$				
7b	60	$(4.16 \pm 0.21) \times 10^{-5}$	70	11.3	24.0	6700							
		$(4.06 \pm 0.21) \times 10^{-5}$											
	70	$(9.08 \pm 0.45) \times 10^{-5}$	60										
		$(9.08 \pm 0.45) \times 10^{-5}$											
	91	$(6.96 \pm 0.45) \times 10^{-4}$	60										
		$(6.90 \pm 0.45) \times 10^{-4}$											

[a] Data taken from ref 24.

chromatography (elution with 5% ethyl acetate in CH_2Cl_2) to give 150 mg (54%) of **5b** as colorless crystals: mp 213 °C (from CH_2Cl_2–hexane); IR (film, cm^{-1}) 1445, 1385, 1150, 1090; ^1H NMR (300 MHz, $CDCl_3$) δ 8.00–7.50 (m, 10 H), 6.06 (dd, J = 1.9, 1.9 Hz, 2 H), 3.80 (s, 2 H), 2.77 (s, 2 H), 2.50 (s, 2 H), 2.20 (dd, J = 1.0, 1.0 Hz, 2 H), 1.73 (d, J = 8.2 Hz, 1 H), 1.48 (d, J = 8.2 Hz, 2 H), 1.25 (m, 1 H), 0.51 (t, J = 8.2 Hz, 2 H); ^{13}C NMR (75 MHz, $CDCl_3$) ppm 142.0, 133.3, 133.1, 128.8, 128.3, 67.6, 59.2, 48.0, 47.9, 43.9, 41.7, 9.4, 4.6; MS m/z (M^+) calcd 466.1272, obsd 466.1269.

For **5a**: colorless crystals, mp 181 °C (60%); IR (film, cm^{-1}) 1450, 1335, 1155, 1085; ^1H NMR (300 MHz, $CDCl_3$) δ 8.00–7.49 (m, 10H), 6.11 (dd, J = 2.0, 2.0 Hz, 2 H), 3.75 (s, 2 H), 3.10 (dd, J = 2.0, 2.0 Hz, 2 H), 2.42 (s, 2 H), 2.37 (s, 2 H), 1.75 (s, 6 H), 1.70 (d, J = 8.2 Hz, 1 H), 1.34 (d, J = 8.2 Hz, 1 H); ^{13}C NMR (75 MHz, $CDCl_3$) ppm 141.6, 140.3, 133.5, 133.2, 128.9, 128.3, 120.0, 65.2, 58.3, 46.3, 44.2, 43.4, 21.0; MS m/z (M^+) calcd 480.1429, obsd 480.1428.

For **10a**: colorless crystals, mp 145–146 °C (from CH_2Cl_2–hexane) (37%); IR (film, cm^{-1}) 1445, 1330, 1200, 1150, 1085; ^1H NMR (300 MHz, $CDCl_3$) δ 8.00–7.53 (m, 10 H), 6.20 (dd, J = 2.2, 2.2 Hz, 2 H), 3.73 (d, J = 2.0 Hz, 2 H), 3.01 (s, 2 H), 2.66 (m, 1 H), 2.64 (s, 2 H), 2.30 (s, 2 H), 1.51 (d, J = 2.4 Hz, 1 H), 1.38 (s, 6 H); ^{13}C NMR (75 MHz, $CDCl_3$) ppm 152.9, 141.2, 133.4, 132.5, 129.0, 128.3, 106.3, 66.9, 47.0, 44.3, 43.45, 43.44, 18.9; MS m/z (M^+) calcd 480.1429, obsd 480.1428.

For **10b**: colorless crystals, mp 219–220 °C dec (from CH_2Cl_2–hexane) (54%); IR (film, cm^{-1}) 1455, 1160, 1090; ^1H NMR (300 MHz, $CDCl_3$) δ 8.01–7.52 (m, 10 H), 6.19 (dd, J = 2.0, 2.0 Hz, 2 H), 3.76 (d, J = 2.0 Hz, 2 H), 2.67 (d, J = 12.0 Hz, 1 H), 2.65 (m, 4 H), 1.88 (s, 2 H), 1.62 (d, J = 12.0 Hz, 1 H), 0.37–0.25 (m, 4 H); ^{13}C NMR (75 MHz, $CDCl_3$) ppm 141.2, 133.4, 133.0, 128.9, 128.4, 67.1, 54.8, 48.9, 48.6, 44.1, 43.3, 8.5, 5.6; MS m/z (M^+) calcd 466.1272, obsd 466.1270.

For **15**: colorless crystals, mp 194 °C (from CH_2Cl_2-hexane) (80%); IR (film, cm^{-1}) 1450, 1335, 1270, 1235, 1150, 1090; ^1H NMR (300 MHz, $CDCl_3$) δ 7.98–7.50 (m, 10 H), 6.16 (s, 2 H), 3.87 (s, 2 H), 2.89 (s, 2 H), 2.23 (s, 2 H), 1.89 (s, 2 H), 1.31 (t, J = 8.0 Hz, 2 H), 0.55 (t, J = 8.0 Hz, 2 H), 0.40–0.30 (m, 4 H); ^{13}C NMR (75 MHz, $CDCl_3$) ppm 142.0, 133.3, 133.1, 128.8, 128.3, 68.1, 48.9, 48.5, 47.8, 41.2, 29.7, 9.3, 8.7, 5.5, 4.7; MS m/z (M^+) calcd 492.1429, obsd 492.1425.

General Procedure for Epoxidation. To a solution of **4a** (500 mg, 1.01 mmol) in cold (0 °C) CH_2Cl_2 (50 mL) was added MCPBA (180 mg, 1.1 mmol) over a 30-min period. The reaction mixture was

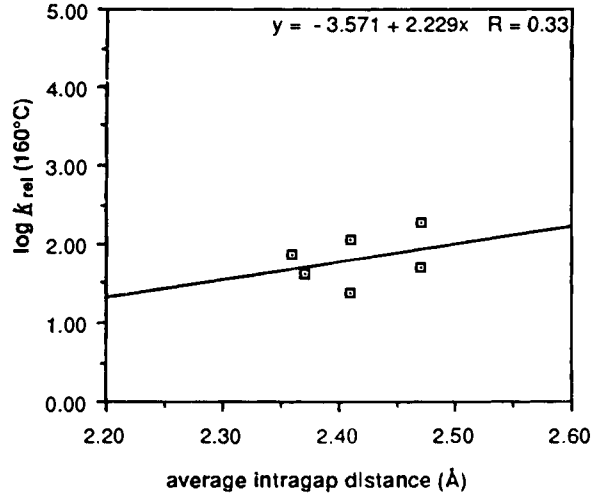

Figure 6. Plot of log k_{rel} (160 °C) versus the average intragap distance (A) for the dihydro disulfones.

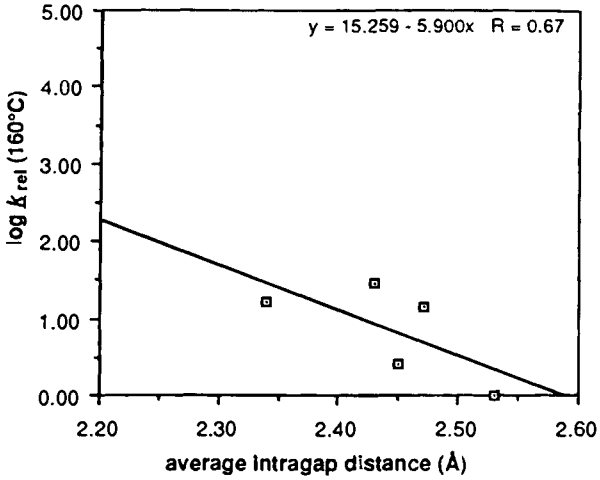

Figure 7. Plot of log k_{rel} (160 °C) versus the average intragap distance for the epoxy disulfones.

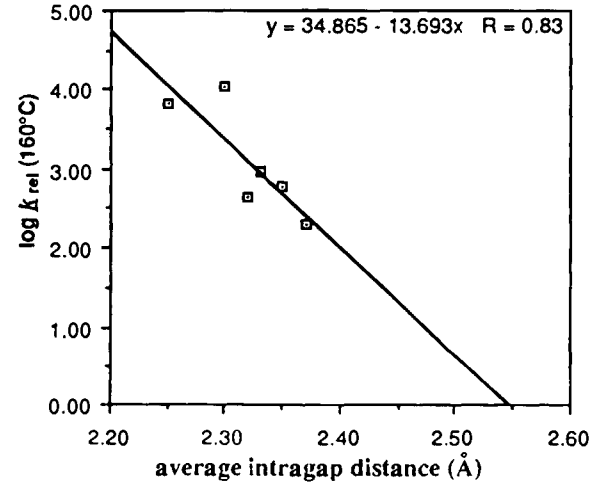

Figure 8. Plot of log k_{rel} (160 °C) versus the average intragap distance for the cyclopropanated disulfones.

stirred overnight, washed sequentially with water (50 mL), 1% NaOH solution (100 mL), and brine (100 mL), dried, and evaporated. The residue was chromatographed on silica gel (elution with 5% ethyl acetate in CH_2Cl_2), and 300 mg (62%) of **6a** was isolated as a colorless crystalline solid: mp 202 °C (from CH_2Cl_2–hexane); IR (film, cm^{-1}) 1445, 1335, 1150, 1085; ^1H NMR (300 MHz, $CDCl_3$) δ 8.01–7.55 (m, 10 H), 6.40 (dd, J = 1.7, 1.7 Hz, 2 H), 3.66 (s, 2 H), 3.62 (d, J = 0.8 Hz, 2 H), 2.89 (s, 2 H), 1.85 (d, J = 8.0 Hz, 1 H), 1.78 (s, 6 H), 1.40 (d, J = 8.0 Hz, 1 H); ^{13}C NMR (50 MHz, $CDCl_3$) ppm 141.0, 139.9, 133.6, 131.8, 129.1, 128.1, 125.8, 65.6, 63.7, 53.3, 45.5, 21.2; MS m/z (M^+) calcd 494.1222, obsd 494.1223.

For **6b**: colorless crystals, mp 213 °C (from CH_2Cl_2-hexane) (65%); IR (film, cm^{-1}) 1395, 1210, 1105; ^1H NMR (300 MHz, $CDCl_3$) δ 7.97–7.50 (m, 10 H), 6.30 (dd, J = 1.8, 1.8 Hz, 2 H), 3.77 (s, 2 H), 2.83 (s, 2 H), 2.74 (s, 2 H), 1.97 (dt, J = 7.9, 1.6 Hz, 1 H), 1.39 (d, J = 7.9 Hz, 1 H), 0.85 (t, J = 8.0 Hz, 2 H), 0.65 (t, J = 8.0 Hz, 2 H); ^{13}C NMR (75 MHz, $CDCl_3$) ppm 141.7, 139.8, 133.5, 129.0, 128.2, 68.3, 65.6, 54.2, 50.0, 44.7, 35.1, 9.3, 5.4; MS m/z (M^+) calcd 480.1065, obsd 480.1051.

For **11a**: colorless crystals, mp 208 °C (from CH_2Cl_2–hexane) (30%); IR (film, cm^{-1}) 1445, 1335, 1155, 1080, 690; ^1H NMR (300 MHz, $CDCl_3$) δ 8.01–7.44 (m, 10 H), 6.54 (dd, J = 1.8, 1.8 Hz, 2 H), 3.72 (d, J = 2.4 Hz, 2 H), 3.43 (s, 2 H) 3.03 (s, 2 H), 2.26 (d, J = 8.9 Hz, 1 H), 1.92 (d, J = 8.9 Hz, 1 H), 1.39 (s, 6 H); ^{13}C NMR (50 MHz, $CDCl_3$) ppm 147.8, 140.7, 140.2, 133.7, 129.1, 128.5, 107.9, 67.0, 64.5, 46.4, 44.0, 35.1, 19.0; MS m/z (M^+) calcd 494.1222, obsd 494.1223.

For **11b:** colorless crystals, mp 238 °C (from CH_2Cl_2–hexane) (65%); IR (film, cm^{-1}) 1445, 1335, 1210, 1155, 1085; ^1H NMR (300 MHz, $CDCl_3$) δ 7.98–7.55 (m, 10 H), 6.50 (dd, J = 1.9, 1.9 Hz, 2 H), 3.78 (d, J = 2.5 Hz, 2 H), 3.01 (s, 2 H), 2.35 (s, 2 H), 2.26 (d, J = 10.8 Hz, 1 H), 1.99 (d, J = 10.8 Hz, 1 H), 0.62 (t, J = 8.0 Hz, 2 H), 0.12 (t, J = 8.0 Hz, 2 H); ^{13}C NMR (75 MHz, $CDCl_3$) ppm 140.5, 139.7, 133.8, 129.1, 128.4, 66.8, 66.0, 52.2, 51.2, 44,2, 35.3, 14.2, 2.7; MS m/z (M^+) calcd 480.1064, obsd 480.1065.

For **16**: colorless crystals, mp 200–201 °C (from CH_2Cl_2–hexane) (69%); IR (film, cm^{-1}) 1445, 1335, 1165, 1085; ^1H NMR (300 MHz, $CDCl_3$) δ 8.06–7.53 (m, 10 H), 6.41 (dd, J = 0.9, 0.9 Hz, 2 H), 3.83 (s, 2 H), 2.76 (s, 2 H), 2.36 (s, 2 H), 1.24 (t, J = 8.4 Hz, 2 H), 0.72–0.65 (m, 4 H), 0.13 (t, J = 8.0 Hz, 2 H); ^{13}C NMR (75 MHz, $CDCl_3$) ppm 141.9, 139.5, 133.5, 129.0, 128.4, 68.2, 66.6, 52.2, 51.5, 50.3, 34.8, 14.5, 9.4, 5.4, 2.8; MS molecular ion too fleeting to be accurately mass measured.

General Procedure for Cyclopropanation. A solution of **4a** (382 mg, 0.80 mmol) in CH_2Cl_2 (25 mL) was treated with excess diazomethane (10 equiv in 100 mL of ether) at 0 °C and stored in a freezer overnight. Residual diazomethane was destroyed by the addition of 1 drop of acetic acid, and the reaction mixture was washed with 10% $NaHCO_3$ solution and brine, filtered through a pad of neutral alumina (activity I), and evaporated. The residue was taken up in CH_2Cl_2 (25 mL) and acetone (5 mL), deoxygenated for 15 min in a quartz cell, and irradiated with a complete bank of 3000 Å lamps in a Rayonet reactor for 30–45 min until no pyrazoline remained. The product cyclopropane was purified by silica gel chromatography (elution with 5% ethyl acetate–CH_2Cl_2) to give 147 mg (38%) of **7a** as a colorless crystalline solid: mp 201 °C (from CH_2Cl_2–hexane); IR (film, cm^{-1}) 1445, 1335, 1150, 1085; ^1H NMR (300 MHz, $CDCl_3$) δ 8.01–7.53 (m, 10 H), 6.33 (dd, J = 1.7, 1.7 Hz, 2 H), 3.88 (s, 3 H), 3.35 (d, J = 0.9 Hz, 2H), 2.63 (s, 2 H), 1.74 (s, 6 H), 1.52 (d, J = 9.6 Hz, 1H), 1.20 (d, J = 7.5 Hz, 1 H), 1.08 (d, J = 9.6 Hz, 1 H), 0.90 (d, J = 7.6 Hz, 1 H); ^{13}C NMR (75 MHz, $CDCl_3$) ppm 141.8, 138.2, 137.3, 133.2, 128.9, 128.1, 124.6, 66.0, 53.7, 45.8, 43.6, 30.7, 21.2, 16.3; MS m/z (M^+) calcd 492.1429, obsd 492.1424.

For **7b**: colorless crystals, mp 218 °C (from CH_2Cl_2–hexane) (80%); IR (film, cm^{-1}) 1450, 1340, 1165, 1095; ^1H NMR (300 MHz, $CDCl_3$) δ 8.00–7.51 (m, 10 H), 6.21 (s, 2 H), 3.96 (s, 2 H), 2.62 (s, 2 H), 2.59 (s, 2 H), 1.98 (d, J = 8.1 Hz, 1 H), 1.67 (d, J = 9.9 Hz, 1 H), 1.50–1.35 (m, 3 H), 1.1 (d, J = 9.8 Hz, 1 H), 0.81 (t, J = 8.3 Hz, 2 H); ^{13}C NMR (62.5 MHz, $CDCl_3$) ppm 142.8, 137.7, 133.1, 128.9, 128.2, 69.6, 54.8, 49.4, 44.0, 38.7, 34.2, 16.1, 13.3, 6.0; MS m/z (M^+) calcd 478.1273, obsd 478.1274.

For **12a**: colorless crystals, mp 195–200 °C (from CH_2Cl_2–hexane) (55%); IR (film, cm^{-1}) 1445, 1325, 1155, 1085; ^1H NMR (300 MHz, $CDCl_3$) δ 7.99–7.53 (m, 10 H), 6.40 (s, 2 H), 3.88 (d, J = 2.4 Hz, 2 H), 3.12 (s, 2 H), 2.78 (s, 2 H), 2.26 (d, J = 12.5 Hz, 1 H), 1.67 (t, J = 12.5 Hz, 1 H), 1.32 (s, 6 H), 1.07 (d, J = 7.7 Hz, 1 H), 0.85 (d, J = 7.7 Hz, 1 H); ^{13}C NMR (75 MHz, $CDCl_3$) ppm 151.5, 141.3, 137.5, 133.5, 129.0, 128.4, 105.7, 67.8, 46.2, 43.4, 38.4, 32.1, 18.9, 15.1; MS m/z (M^+) calcd 492.1429, obsd 492.1426.

For **12b**: colorless crystals, mp 205 °C (from CH_2Cl_2–hexane) (78%); IR (film, cm^{-1}) 1445, 1335, 1150, 1085; ^1H NMR (300 MHz,

$CDCl_3$)δ 7.97−7.53 (m, 10 H), 6.44 (s, 2 H), 3.96 (d, J = 2.4 Hz, 2 H), 2.78 (s, 2 H), 2.27 (d, J = 12.5 Hz, 1 H), 2.10 (d, J = 7.9 Hz, 1 H), 2.07 (s, 2 H), 1.79 (d, J = 12.7 Hz, 1 H), 1.04 (d, J = 7.9 Hz, 1 H), 0.67 (t, J = 8.0 Hz, 2 H), 0.08 (t, J = 8.0 Hz, 2 H); ^{13}C NMR (75 MHz, $CDCl_3$) ppm 141.1, 138.2, 133.4, 128.9, 128.3, 67.5, 52.5, 50.1, 43.8, 38.3, 34.6, 18.6, 14.0, 5.1; MS *m/z* (M^+) calcd 478.1273, obsd 478.1269.

For **17**: colorless crystals, mp 120−125 °C (from CH_2Cl_2-hexane) (83%); IR (film, cm^{-1}) 1445, 1325, 1155, 1085; ^{1}H NMR (300 MHz, $CDCl_3$) δ 7.99−7.50 (m, 10 H), 6.31 (dd, J = 1.8, 1.8 Hz, 2 H), 3.99 (s, 2 H), 2.57 (s, 2 H), 2.21 (d, J = 7.2 Hz, 2 H), 2.05 (s, 2 H), 1.40 (t, J = 7.5 Hz, 2 H), 0.86 (t, J = 7.5 Hz, 2 H), 0.70 (t, J = 8.0 Hz, 2 H), 0.13 (t, J = 8.0 Hz, 2 H); ^{13}C NMR (75 MHz, $CDCl_3$) ppm 142.8, 137.6, 133.1, 128.9, 128.2, 69.3, 52.4, 50.3, 49.4, 37.8, 35.8, 18.9, 17.5, 12.9, 5.8, 5.2; MS *m/z* (M^+) calcd 504.1429, obsd 504.1420.

General Dyotropic Rearrangement Procedure. A. Dihydro Disulfone 5a. A solution of **5a** (20 mg, 0.41 mmol) in 15 mL of bromobenzene was heated at 120 °C for 48 h under argon. The bromobenzene was removed in vacuo, and the residue was submitted to MPLC purification (silica gel, elution with 2.5% ethyl acetate in CH_2Cl_2). There was obtained 10 mg (50%) of **19a** as a white solid: mp 200 °C (from CH_2Cl_2−hexane); IR (film, cm^{-1}) 1450, 1335, 1160, 1090; ^{1}H NMR (300 MHz, $CDCl_3$) δ 7.64−7.35 (m, 10 H), 3.54 (dd, J = 1.9, 1.9 Hz, 2 H), 2.56 (s, 2 H), 2.28 (s, 2 H), 1.5 (m, 6 H), 1.06 (s, 6 H); ^{13}C NMR (75 MHz, $CDCl_3$) ppm 152.59, 152.56, 140.0, 133.6, 129.0, 128.3, 108.8, 51.5, 49.3, 46.9, 39.2, 25.5, 17.9; MS *m/z* (M^+) calcd 480.1429, obsd 480.1427.

Anal. Calcd for $C_{27}H_{28}O_4S_2$: C, 67.47; H, 5.87. Found: C, 67.03; H, 6.04.

B. Dihydro Disulfone 5b. 5b (10 mg, 0.21 mmol) in 15 mL of bromobenzene; 120 °C for 24 h; silica gel chromatography gave 9 mg (90%) of **19b** as a colorless solid: mp 227 °C (from CH_2Cl_2−hexane); IR (film, cm^{-1}) 1445, 1395, 1210, 1160, 1090; ^{1}H NMR (300 MHz, $CDCl_3$) δ 7.78−7.47 (m, 10 H), 2.81 (d, J = 1.6 Hz, 2 H), 2.48 (dd, J = 1.9, 1.9 Hz, 2 H), 2.27 (s, 2 H), 1.67 (d, J = 9.4 Hz, 1 H), 1.56 (m, 1 H), 1.53 (m, 4 H), 0.26 (t, J =7.9 Hz, 2 H), −0.30 (t, J = 7.9Hz, 2 H); ^{13}C NMR (62.5 MHz, $CDCl_3$, ppm) 153.7, 139.9, 133.9, 128.9, 65.8, 58.8, 55.6, 50.6, 47.5, 39.0, 25.8, 8.8, 4.9; MS *m/z* (M^+) calcd 466.1272, obsd 466.1265.

Anal. Calcd for $C_{26}H_{26}O_4S_2$: C, 66.93; H, 5.62. Found: C, 66.85; H, 5.84.

C. Epoxy Disulfone 6a. 6a (20 mg, 0.40 mmol) in 15 mL of bromobenzene; 160 °C for 24 h; silica gel chromatography gave 12 mg (60%) of **20a** as a colorless solid: mp 222 °C dec (from CH_2Cl_2−hexane); IR (film, cm^{-1}) 1445, 1335, 1150, 1085; ^{1}H NMR (300 MHz, $CDCl_3$) δ 7.82−7.46 (m, 10 H), 3.98 (s, 2 H), 2.74 (s, 2 H), 1.85 (d, J = 1.6 Hz, 1 H), 1.68−1.59 (m, 5 H), 1.54 (s, 6 H); ^{13}C NMR (62.5 MHz, $CDCl_3$) ppm 158.9, 148.4, 139.2, 134.2, 129.2, 128.6, 110.6, 64.6, 54.0, 39.3, 38.9, 25.1, 18.1; MS *m/z* (M^+) calcd 494.1222, obsd 494.1223.

Anal. Calcd for $C_{27}H_{26}O_5S_2$: C, 65.56; H, 5.30. Found: C, 65.16; H, 5.34.

D. Epoxy Disulfone 6b. 6b (10 mg, 0.21 mmol) in 15 mL of bromobenzene; 160 ° C for 24 h; silica gel chromatography gave 8.5 mg (85%) of **20b** as a colorless solid: mp 236 °C (from CH_2Cl_2−hexane); IR (film, cm^{-1}) 1445, 1325, 1160, 1090; ^{1}H NMR (300 MHz, $CDCl_3$) δ 7.85−7.50 (m, 10 H), 2.96 (s, 2 H), 2.70 (s, 2 H), 1.90 (d, J = 9.5 Hz, 1 H), 1.7−1.4 (m, 4 H), 0.96 (d, J = 9.5 Hz, 1 H), 0.57 (t, J = 8.3 Hz, 2 H), −0.54 (t, J = 8.3 Hz, 2 H); ^{13}C NMR (50 MHz, $CDCl_3$) ppm 159.4, 139.1, 134.4, 129.2 (2 C), 66.1, 58.3, 56.2, 39.6, 39.4, 25.0, 14.2, 1.3; MS *m/z* (M^+) calcd 480.1065, obsd 480.1069.

Anal. Calcd for $C_{26}H_{24}O_5S_2$: C, 64.98; H, 5.03. Found: C, 65.04; H, 5.10.

E. Cyclopropanated Disulfone 7a. 7a (20 mg, 0.41 mmol) in 15 mL of bromobenzene; 120 °C for 24 h; silica gel chromatography gave 10 mg (50%) of **21a** as a colorless solid: mp 234.5 °C (from CH_2Cl_2−hexane); IR (film, cm^{-1}) 1440, 1335, 1155, 1090; ^{1}H NMR (300 MHz, $CDCl_3$) δ 7.65−7.41 (m, 10 H), 3.70 (s, 2 H), 2.47 (s, 2 H), 2.17 (d, J = 5.4 Hz, 1 H), 1.63−1.58 (m, 5 H), 0.98 (d, J = 7.5 Hz, 1 H), 0.92 (s, 6 H), 0.73 (d, J = 7.6 Hz, 1 H); ^{13}C NMR (75 MHz, $CDCl_3$) ppm 156.9, 151.5, 139.7, 133.8, 129.0, 128.6, 108.9, 54.1, 42.3, 38.4, 32.7, 27.4, 17.9, 13.9; MS *m/z* (M^+) calcd 492.1429 obsd 492.1423.

Anal. Calcd for $C_{28}H_{28}O_4S_2$: C, 68.27; H, 5.73. Found: C, 68.14; H, 5.66.

F. Cyclopropanated Disulfone 7b. 7b (10 mg, 0.21 mmol) in 15 mL of bromobenzene; 100 °C for 24 h, silica gel chromatography gave 9 mg (90%) of **21b** as a white solid: mp 218 °C (from CH_2Cl_2−hexane); IR (film, cm^{-1}) 1449, 1385, 1175, 1090; ^{1}H NMR (300 MHz, $CDCl_3$) δ 8.00−7.51 (m, 10 H), 2.71 (s, 2 H), 2.40 (s, 2 H), 1.76 (d, J = 7.8 Hz, 1 H), 1.70 (d, J = 10.9 Hz, 1 H), 1.55 (m, 4 H), 1.05 (d, J = 7.7 Hz, 1 H), 0.93 (d, J = 10.9 Hz, 1 H), 0.57 (t, J = 8.3 Hz, 2 H), −0.63 (t, J = 8.3 Hz, 2 H); ^{13}C NMR (75 MHz, $CDCl_3$) ppm 158.8, 139.6, 134.1, 129.5, 129.1, 57.8, 56.3, 42.5, 39.0, 35.2, 27.4, 18.3, 13.5, 2.8; MS *m/z* (M^+) calcd 478.1273, obsd 478.1268.

Anal. Calcd for $C_{27}H_{26}O_4S_2$: C, 67.47; H, 5.87. Found: C, 67.50; H, 5.57.

G. Dihydro Disulfone 10a. 10a (20 mg, 0.41 mmol) in 15 mL of bromobenzene; 120 °C for 48 h; silica gel chromatography gave 11 mg (55%) of **22a** as a colorless solid: mp 171 °C (from CH_2Cl_2−hexane); IR (film, cm^{-1}) 1450, 1335, 1155, 1085; ^{1}H NMR (300 MHz, $CDCl_3$) δ 8.00−7.49 (m, 10 H), 3.11 (s, 2 H), 2.68 (s, 2 H), 2.63 (s, 2 H), 1.74 (d, J = 8.6 Hz, 1 H), 1.61 (s, 6 H), 1.55 (s, 2 H) 1.51 (s, 2 H), 1.6−1.5 (m, 1 H); ^{13}C NMR (75 MHz, $CDCl_3$) ppm 154.4, 148.2, 140.3, 133.9, 129.1, 128.7, 112.6, 61.8, 51.0, 48.0, 38.9, 24.4, 20.3; MS *m/z* (M^+) calcd 480.1429, obsd 480.1427.

Anal. Calcd for $C_{27}H_{28}O_4S_2$: C, 67.47; H, 5.87. Found: C, 67.08; H, 5.88.

H. Dihydro Disulfone 10b. 10b (10 mg, 0.21 mmol) in 15 mL of bromobenzene; 120 °C for 48 h; silica gel chromatography gave 6 mg (60%) of **22b** as a colorless solid: mp 195−197 °C dec (from CH_2Cl_2−hexane); IR (film, cm^{-1}) 1450, 1325, 1160, 1090; ^{1}H NMR (300 MHz, $CDCl_3$) δ 7.85−7.81 (m, 4 H), 7.68−7.62 (m, 2 H), 7.53−7.44 (m, 4 H), 3.11 (d, J = 1.5 Hz, 2 H), 2.93 (d, J = 1.3 Hz, 2 H), 1.81−1.52 (m, 4 H), 1.45 (s, 2 H), 0.58−0.40 (m, 6 H); ^{13}C NMR (75 MHz, $CDCl_3$) ppm 154.9, 140.4, 133.9, 129.1, 128.7, 62.6, 50.9, 50.0, 44.0, 43.5, 25.6, 5.6, 5.2; MS *m/z* (M^+) calcd 466.1272, obsd 466.1269.

Anal. Calcd for $C_{28}H_{28}O_4S_2$: C, 66.93; H, 5.62. Found: C, 66.64; H, 5.70.

I. Epoxy Disulfone 11a. 11a (20 mg, 0.40 mmol) in 15 mL of bromobenzene; 160 °C for 24 h; silica gel chromatography gave 5 mg (25%) of **23a** as a colorless solid: mp 206 °C (from CH_2Cl_2−hexane); IR (film, cm^{-1}) 1440, 1330, 1150, 1085; ^{1}H NMR (300 MHz, $CDCl_3$) δ 7.85−7.50 (m, 10 H), 3.48 (s, 2 H), 3.22 (s, 2 H), 1.99 (d, J = 8.5 Hz, 1 H), 1.71 (d, J = 4.9 Hz, 1 H), 1.56 (s, 6 H), 1.7−1.40 (m, 4 H); ^{13}C NMR (50 MHz, $CDCl_3$) ppm 159.8, 139.8, 139.4, 134.4, 129.4, 128.7, 115.4, 64.0, 56.5, 51.8, 41.3, 24.5, 19.9; MS *m/z* (M^+) calcd 494.1222, obsd 494.1221.

Anal. Calcd for $C_{27}H_{26}O_5S_2$: C, 65.56; H, 5.30. Found: C, 65.10; H, 5.35.

J. Epoxy Disulfone 11b. 11b (20 mg, 0.21 mmol) in 15 mL of bromobenzene; 160 °C for 24 h; silica gel chromatography gave 13 mg (65%) of **23b** as a colorless solid: mp 235 °C (from CH_2Cl_2−hexane); IR (film, cm^{-1}) 1445, 1335, 1165, 1035; ^{1}H NMR (300 MHz, $CDCl_3$) δ 7.75−7.42 (m, 10 H), 3.37 (s, 2 H), 2.01 (d, J = 1.3 Hz, 1 H), 1.89 (s, 2 H), 1.70 (d, J = 10.7 Hz, 2 H), 1.45 (d, J = 9.9 Hz, 2 H), 1.32 (d, J = 8.4 Hz, 1 H), 0.60 (t, J = 7.9 Hz, 2 H), 0.09 (t, J = 7.9 Hz, 2 H); ^{13}C NMR (75 MHz, $CDCl_3$) ppm 159.7, 139.4, 134.4, 129.3, 128.6, 65.9, 57.0, 52.0, 45.7, 37.7, 25.3, 10.9, 2.3; MS *m/z* (M^+) calcd 480.1064, obsd 480.1065.

Anal. Calcd for $C_{26}H_{24}O_5S_2$: C, 64.98; H, 5.03. Found: C, 64.94; H, 5.09.

K. Cyclopropanated Disulfone 12a. Heating of **12a** in bromobenzene at 120 °C during 24 h promoted its decomposition; only a trace of the presumed dyotropic product was detected by TLC.

L. Cyclopropanated Disulfone 12b. 12b (10 mg, 0.21 mmol) in 15 mL of bromobenzene; 120 °C for 24 h; silica gel chromatography gave 5.5 mg (55%) of **24b** as a colorless solid: mp 215−216 °C dec (from CH_2Cl_2−hexane); IR (film, cm^{-1}) 1445, 1325, 1155, 1090; ^{1}H NMR (300 MHz, $CDCl_3$) δ 7.83−7.47 (m, 10 H), 3.23 (s, 2 H), 1.92 (d, J = 7.9 Hz, 1 H), 1.78−1.58 (m, 4 H), 1.05 (d, J = 10.9 Hz, 1 H), 0.9−0.8 (m, 4 H), 0.76 (t, J = 7.8 Hz, 2H), 0.24 (t, J = 7.8 Hz, 2 H);

^{13}C NMR (75 MHz, $CDCl_3$) ppm 158.9, 140.1, 133.9, 129.1, 128.7, 57.1, 51.6, 44.6, 34.8, 27.7, 22.3, 14.5, 13.2, 4.2; MS *m/z* (M^+) calcd 492.1429, obsd 492.1424.

Anal. Calcd for $C_{27}H_{26}O_4S_2$: C, 67.47 H, 5.87. Found: C, 67.14; H, 5.54.

M. Dihydro Disulfone 15. **15** (10 mg, 0.20 mmol) in 15 mL of bromobenzene; 120 °C for 24 h; silica gel chromatography gave 9 mg (90%) of **25** as a colorless solid: mp 194 °C (from CH_2Cl_2–hexane); IR (film, cm^{-1}) 1445, 1320, 1270, 1160, 1090; ^{1}H NMR (300 MHz, $CDCl_3$) δ 7.78–7.46 (m, 10 H), 3.06 (s, 2 H), 2.50 (dd, J =1.8, 1.8 Hz, 2 H), 1.8–1.7 (m, 2 H), 1.67–1.60 (m, 2 H), 1.49 (s, 2 H), 0.60–0.42 (m, 4 H), 0.30 (t, J = 7.8 Hz, 2 H), −0.28 (t, J = 7.8 Hz, 2 H); ^{13}C NMR (20 MHz, $CDCl_3$) ppm 154.4, 139.9, 133.9, 128.9 (2 C), 58.3, 55.8, 50.7, 44.0, 43.2, 26.2, 8.9, 5.7, 5.0, 4.8; MS *m/z* (M^+) calcd 492.1429, obsd 492.1411.

Anal. Calcd for $C_{28}H_{28}O_4S_2$: C, 68.27; H, 5.73. Found: C, 68.33; H, 5.81.

N. Epoxy Disulfone 16. **16** (10 mg, 0.20 mmol) in 15 mL of bromobenzene; 160 °C for 24 h; silica gel chromatography gave 9 mg (90%) of **26** as a colorless solid: mp 190–195 °C dec (from CH_2Cl_2–hexane); IR (film, cm^{-1}) 1450, 1340, 1165, 1095; ^{1}H NMR (300 MHz, $CDCl_3$) δ 7.87–7.51 (m, 10 H), 2.99 (s, 2 H), 2.00 (s, 2 H), 1.78 (d, J = 11.0 Hz, 2 H), 1.54 (d, J = 11.0 Hz, 2 H), 0.71 (t, J = 7.7 Hz, 2 H), 0.62 (t, J = 8.3 Hz, 2 H), 0.19 (t, J = 7.7 Hz, 2 H), −0.51 (t, J = 8.3 Hz, 2 H); ^{13}C NMR (75 MHz, $CDCl_3$) ppm 159.3, 139.1, 134.4, 129.3, 129.2, 67.1, 58.7, 55.8, 46.0, 37.2, 25.8, 14.3, 10.9, 2.2, 1.2; MS *m/z* (M^+) calcd 506.1222, obsd 506.1220.

Anal. Calcd for $C_{28}H_{26}O_5S_2$: C, 66.38; H, 5.17. Found: C, 66.12; H, 5.14.

O. Cyclopropanated Disulfone 17. **17** (10 mg, 0.20 mmol) in 15 mL of bromobenzene; 100 °C for 24 h; silica gel chromatography gave 9 mg (90%) of **27** as a colorless solid: mp 241 °C (from CH_2Cl_2–hexane); IR (film, cm^{-1}) 1449, 1330, 1155, 1090; ^{1}H NMR (300 MHz, $CDCl_3$) δ 8.00–7.50 (m, 10 H), 2.70 (s, 2 H), 1.93 (d, J = 10.2 Hz, 2 H), 1.80 (d, J = 10.2 Hz, 2 H), 1.65 (m, 4 H), 0.75 (t, J = 8.3 Hz, 2 H), 0.60 (t, J = 8.3 Hz, 2 H), 0.25 (t, J = 8.3 Hz, 2 H), −0.65 (t, J = 8.3 Hz, 2 H); ^{13}C NMR (75 MHz, $CDCl_3$) ppm 158.8, 139.5, 134.1, 129.4, 129.0, 58.0, 55.4, 44.7, 39.8, 36.7, 27.4, 18.0, 15.0, 14.2, 4.0, 2.6; MS *m/z* (M^+) calcd 504.1429, obsd 504.1442.

Anal. Calcd for $C_{29}H_{28}O_4S_2$: C, 69.02; H, 5.59. Found: C, 69.14; H, 5.69.

Kinetic Measurements. The dyotropic rearrangements were performed in degassed C_6D_5Br solutions and followed by either 250 or 300 MHz ^{1}H NMR. The particular signals that were integrated for the starting materials, and products were standardized to reference samples containing authentic 50:50 distributions of the pair of compounds. A minimum of five data points were taken for each kinetic run, which was performed in duplicate. The heating of the samples was performed by one of two methods:

Method A: the C_6D_5Br solution was heated in a thermostated oil bath. At intervals, the samples were removed, quickly cooled to 0 °C, and maintained at this temperature until the ^{1}H NMR spectrum was taken soon thereafter.

Method B: The C_6D_5Br solution was placed in a NMR tube and heated directly in the probe of the NMR spectrometer at the desired temperature. ^{1}H NMR spectra were recorded at regular intervals.

In three instances, rates were determined by both methods and the correspondence was found to be identical within the limits of experimental error.

Care was taken to establish that all of the rearrangements were first-order. In several examples, the substrate concentration was varied from 1–10 mg/mL and no variation in the initial rates was observed. Consequently, the reported k_{obs} are in fact k_f and not values contaminated with k_r as

$$k = k_f + k_r = k_f(1 + K_{eq}^{-1})$$

The kinetic measurements involved quantifying both SM + P[C] versus time and then plotting a least-squares fit of ln[%SM] versus time to obtain k_f. Knowledge of K_{eq} permitted calculation of k_r. The accuracy of the K_{eq} values are high for those that fall in the range of 1–10, somewhat less accurate when between 10–20, and only roughly approximate when > 20.

Acknowledgment. We are grateful to the National Institutes of Health for financial support of this work (Grant CA-12115).

Supplementary Material Available: Summary of data collection and data refinement, crystallographic experimental details, and tables of bond distances, final fractional coordinates, thermal parameters, and least-squares planes for the 16 compounds described in Figures 1–4 (189 pages); tables of structure factors (94 pages). This material is contained in many libraries on microfiche, immediately follows this article in the microfilm version of the journal, and can be ordered from the ACS; see any current masthead page for ordering information.